

**Electronic Supplementary Information**

**Investigation of local structure distortion and electron cloud interaction on  
emission-band broadening induced by concentration-perturbation effect of cation  
substituting in BaY<sub>2</sub>Si<sub>3</sub>O<sub>10</sub>:Eu phosphors**

Haoran Li<sup>a</sup>, Yujun Liang<sup>a,\*</sup>, Yingli Zhu<sup>a</sup>, Shiqi Liu<sup>a</sup>, Jiahui Chen<sup>a</sup>, Hang Zhang<sup>a</sup>, Yongjun Chen<sup>b</sup>

<sup>a</sup>Engineering Research Center of Nano-Geomaterials of Ministry of Education, Faculty of Materials Science and Chemistry, China University of Geosciences, Wuhan 430074, China, *E-mail:* [yujunliang@sohu.com](mailto:yujunliang@sohu.com)

<sup>b</sup>State Key Laboratory of Marine Resource Utilization in South China Sea, School of Materials Science and Engineering, Hainan University, Haikou 570228, China

\*Corresponding Author: [yujunliang@sohu.com](mailto:yujunliang@sohu.com)(Y. Liang).

Table S1 The cell parameters and reliability factors for BYSO:Eu,  $(x/y/z)M^{2+}$  ( $M = Mn$ ,  $x = 0.0\%-6.0\%$ ;  $M = Mg$ ,  $y = 0.0\%-5.0\%$ ,  $M = Zn$ ,  $z = 0.0\%-20.0\%$ , respectively)

Mn	a (Å)	b (Å)	c (Å)	V (Å <sup>3</sup> )	R <sub>p</sub>	R <sub>wp</sub>	R <sub>exp</sub>	χ <sup>2</sup>
0.0%	5.38941(13)	12.18531(30)	6.84419(15)	431.186(18)	5.47	7.22	3.07	5.55
0.2%	5.39255(15)	12.19283(36)	6.85010(18)	432.120(21)	5.47	7.48	3.12	5.76
0.4%	5.39377(15)	12.19208(37)	6.85052(19)	432.221(22)	5.53	7.38	3.16	5.46
0.6%	5.39324(15)	12.19249(37)	6.85053(19)	432.193(22)	5.71	7.76	3.08	6.37
0.8%	5.3935(16)	12.19189(39)	6.85011(20)	432.168(23)	5.28	7.15	3.08	5.38
1.0%	5.3938(16)	12.19197(37)	6.85051(19)	432.221(22)	5.62	7.54	3.08	6.00
2.0%	5.39375(16)	12.19087(39)	6.85023(20)	432.164(23)	5.24	7.03	3.10	5.13
3.0%	5.39251(14)	12.19145(38)	6.84958(18)	432.037(20)	5.05	6.84	3.02	5.13
4.0%	5.39273(14)	12.19597(36)	6.85027(19)	432.257(22)	5.2	7.16	3.08	5.40
5.0%	5.39406(15)	12.19833(35)	6.85200(18)	432.549(21)	4.92	6.75	3.10	4.74
6.0%	5.39291(14)	12.1916(33)	6.84949(17)	432.069(19)	5.01	6.79	2.89	5.51
Mg	a (Å)	b (Å)	c (Å)	V (Å <sup>3</sup> )	R <sub>p</sub>	R <sub>wp</sub>	R <sub>exp</sub>	χ <sup>2</sup>
0.5%	5.39226(14)	12.1917(34)	6.84929(18)	432.007(20)	4.56	6.28	3.02	4.33
1.0%	5.39232(17)	12.19132(43)	6.84893(22)	431.977(25)	5.12	7.16	2.97	5.80
1.5%	5.3926(16)	12.1887(38)	6.84879(20)	431.905(22)	4.79	6.71	2.93	5.25
2.0%	5.39152(19)	12.18876(48)	6.84812(25)	431.776(28)	5.23	7.82	2.99	6.84
3.0%	5.3921(15)	12.19274(37)	6.84914(19)	432.027(22)	4.54	6.44	3.00	4.59
4.0%	5.39177(18)	12.19024(34)	6.84849(23)	431.865(25)	5.04	7.48	3.02	6.15
5.0%	5.39336(14)	12.19651(34)	6.85102(18)	432.370(20)	4.42	6.10	3.02	4.08
Zn	a (Å)	b (Å)	c (Å)	V (Å <sup>3</sup> )	R <sub>p</sub>	R <sub>wp</sub>	R <sub>exp</sub>	χ <sup>2</sup>
1.00%	5.3941(15)	12.19037(36)	6.85035(18)	432.182(21)	5.03	6.99	2.93	5.71
3.00%	5.39339(13)	12.18676(32)	6.8493(17)	431.929(19)	4.92	6.88	2.93	5.51
5.00%	5.39327(14)	12.18908(34)	6.84956(18)	432.020(20)	4.78	6.72	2.90	5.37
7.00%	5.39302(16)	12.18977(39)	6.84955(20)	432.017(23)	5.26	7.36	2.94	6.28
10.00%	5.39385(14)	12.18859(33)	6.84989(17)	432.070(19)	5.18	7.17	2.98	5.77
15.00%	5.39371(15)	12.18862(37)	6.84994(19)	432.062(22)	5.06	7.45	2.94	6.43
20.00%	5.39246(18)	12.18933(45)	6.84882(23)	431.925(26)	5.18	7.69	2.86	7.21

Table S2 The distortion index, D, bond length and average  $U_{iso,i}$  values for BYSO:Eu,  $x$ Mn ( $x = 0.0\%-6.0\%$ )

Concentration (mol)		0.0%	0.2%	0.4%	0.6%	0.8%	1.0%	2.0%	3.0%	4.0%	5.0%	6.0%
D	[BaO <sub>8</sub> ]	0.0377	0.0380	0.0552	0.0534	0.0549	0.0517	0.0609	0.0471	0.0459	0.0394	0.0398
	[YO <sub>6</sub> ]	0.0200	0.0196	0.0164	0.0174	0.0123	0.0176	0.0234	0.0141	0.0161	0.0172	0.0156
Bond length	Ba-O	2.8696	2.8720	2.8505	2.8454	2.8077	2.8521	2.8240	2.8368	2.8449	2.8575	2.8713
Average [BaO <sub>8</sub> ]		0.50004	0.601	0.315	0.547	0.691	0.539	0.352	0.420	0.116	0.325	0.792
U <sub>iso</sub> [YO <sub>6</sub> ]		0.50006	0.824	0.921	1.134	1.072	1.262	1.375	0.731	0.810	0.395	1.323

Table S3 The distortion index, D, bond length and average  $U_{iso,i}$  values for BYSO:Eu,  $y$ Mg ( $y = 0.0\%-5.0\%$ )

Concentration (mol)	0.0%	0.5%	1.0%	1.5%	2.0%	3.0%	4.0%	5.0%
D	[BaO <sub>8</sub> ]	0.0377	0.0464	0.0565	0.0437	0.0606	0.0434	0.0538
	[YO <sub>6</sub> ]	0.0200	0.0125	0.0343	0.0260	0.0319	0.0232	0.0235
Bond length	Ba-O	2.8696	2.8641	2.8653	2.8914	2.8885	2.8824	2.8820
	Y-O	2.2664	2.2800	2.2702	2.2495	2.2621	2.2673	2.2591
Average [BaO <sub>8</sub> ]	0.50004	0.613	1.451	1.212	0.917	0.773	0.715	0.648
$U_{iso}$ [YO <sub>6</sub> ]	0.50006	1.860	1.393	1.842	1.979	1.640	1.610	1.902

Table S4 The distortion index, D, bond length and average  $U_{iso,i}$  values for BYSO:Eu,  $z$ Zn ( $z = 0.0\%-20.0\%$ )

Concentration (mol)	0.0%	1.0%	3.0%	5.0%	7.0%	10.0%	15.0%	20.0%
D	[BaO <sub>8</sub> ]	0.0377	0.0510	0.0403	0.0426	0.0530	0.0448	0.0413
	[YO <sub>6</sub> ]	0.0200	0.0228	0.0241	0.0193	0.0259	0.0250	0.0204
Bond length	Ba-O	2.8696	2.8704	2.8656	2.8547	2.8880	2.8756	2.8656
	Y-O	2.2664	2.2791	2.2598	2.2673	2.2582	2.2677	2.2717
Average [BaO <sub>8</sub> ]	0.50004	0.966	1.100	0.951	1.846	0.903	0.958	1.223
$U_{iso}$ [YO <sub>6</sub> ]	0.50006	1.895	1.697	1.952	1.806	1.575	1.954	1.528

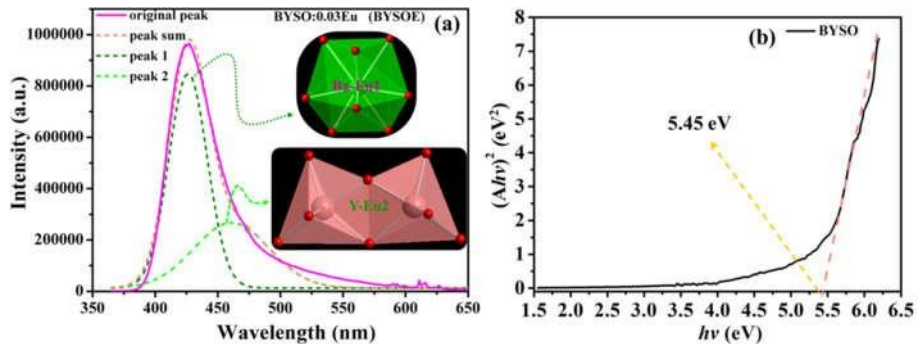


Figure S1. The Gaussian peaks fitting of BYSO:Eu at Ba-Eu(1) site (peaking at 429 nm) and Y-Eu(2) site (peaking at 475 nm) under  $\lambda_{ex} = 323$  nm (a); the plots of  $(Ahv)^2$  versus  $hv$  of BYSO host (b).

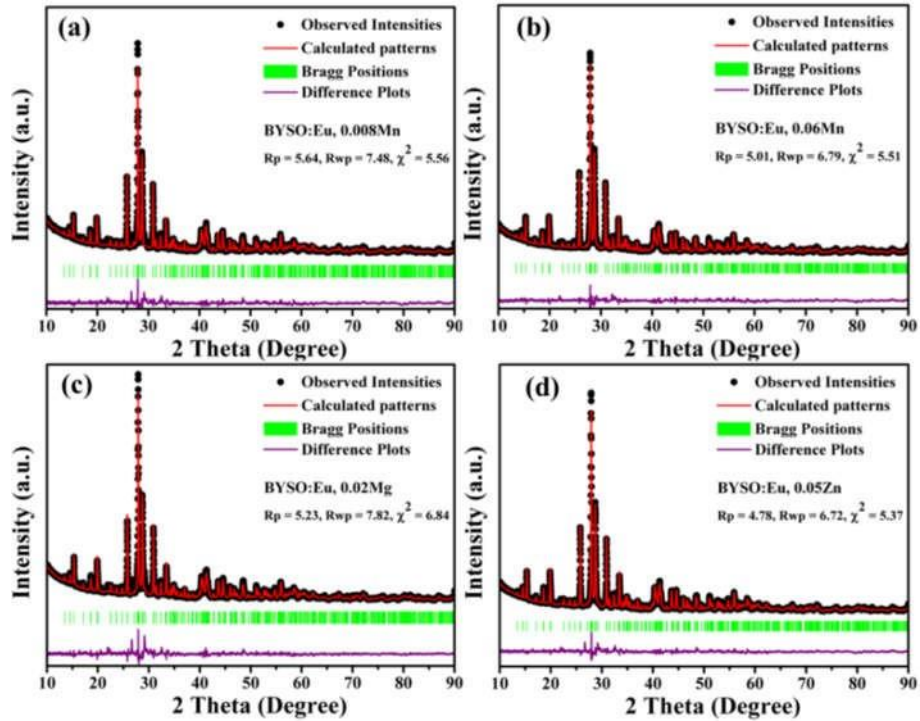


Figure S2. Rietveld refinements results for representative BYSO:Eu, 0.008Mn (a), BYSO:Eu, 0.06Mn (b), BYSO:Eu, 0.02Mg (c) and BYSO:Eu, 0.05Zn (d) using FullProf. program.

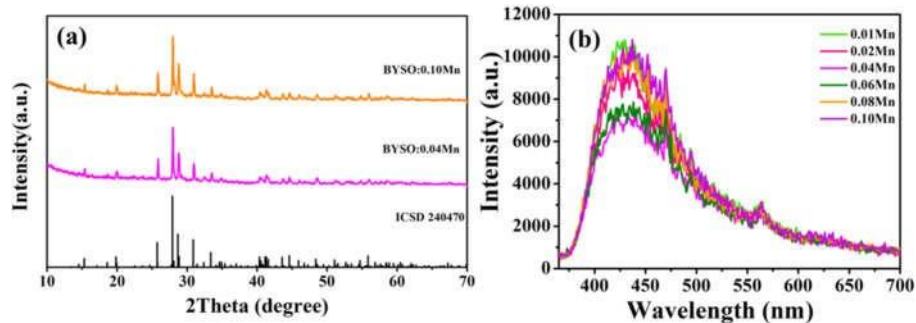


Figure S3. XRD patterns of BYSO:  $m$ Mn,  $m = 0.00-0.10$  and the standard reference for BYSO (ICSD 240470) (a), PL spectra of BYSO:  $m$ Mn,  $m = 0.00-0.10$ .

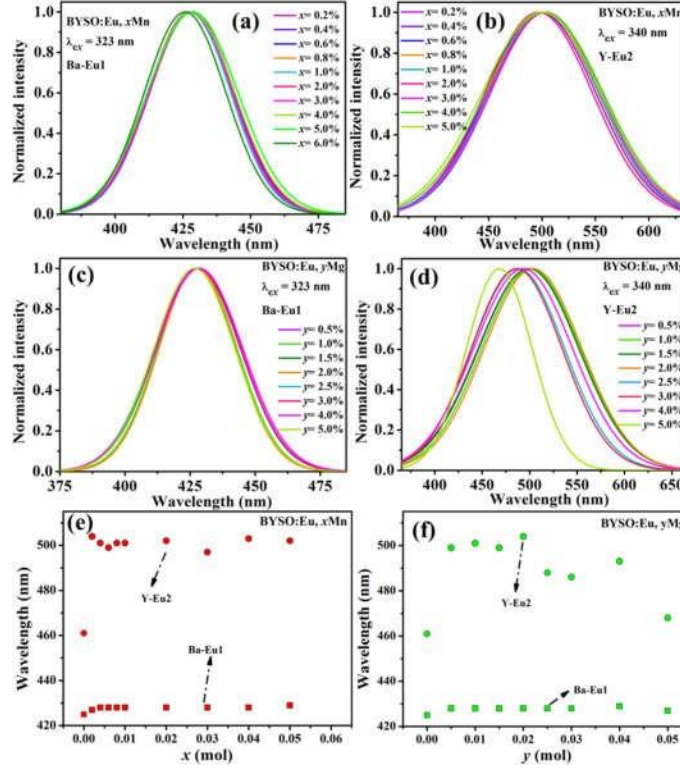


Figure S4. The PL spectra are decomposed into Gaussian contributions from Eu<sup>2+</sup> at the two cation sites in the BYSO:Eu,  $(x/y)\text{M}^{2+}$ : M = Mn,  $x$  = 0.2%-6.0%, Eu<sup>2+</sup> at the Ba<sup>2+</sup> sites (a), Eu<sup>2+</sup> at the Y<sup>3+</sup> sites (b); M = Mg,  $y$  = 0.5%-5.0%, Eu<sup>2+</sup> at the Ba<sup>2+</sup> sites (c), Eu<sup>2+</sup> at the Y<sup>3+</sup> sites (d); emission peak shifts of Eu1 and Eu2 for BYSO:Eu,  $x$ Mn<sup>2+</sup> (e) and BYSO:Eu,  $y$ Mg<sup>2+</sup> (f).

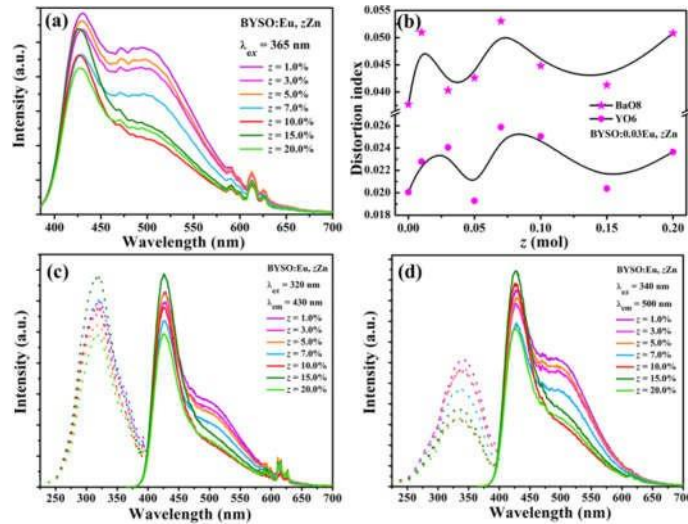


Figure S5. PL spectra of BYSO:Eu,  $z$ Zn samples excited at  $\lambda_{ex} = 365$  nm at room temperature ( $z$  = 1.0%-20.0%) (a); the distortion index, D, along with  $z$  for [BaO<sub>8</sub>] polyhedra and [YO<sub>6</sub>] octahedra of BYSO:Eu,  $z$ Zn (b) samples; PLE and PL spectra of BYSO:Eu,  $z$ Zn ( $z$  = 1.0%-20.0%) samples at room temperature:  $\lambda_{ex} = 320$  nm &  $\lambda_{em}$  = 430 nm (c),  $\lambda_{ex} = 340$  nm &  $\lambda_{em}$  = 500 nm (d).

Figure S5 shows the PL spectra of BYSO:Eu,  $z$ Zn samples, which also reveal series of broad emission bands due to the enhancement of second emission peak when excited at 365 nm. The emission intensities reach the maximum value at  $z = 1.0$  mol % for BYSO:Eu,  $z$ Zn. And for BYSO:Eu,  $z$ Zn, the distortion index for both [BaO<sub>8</sub>] and [YO<sub>6</sub>] increase roughly as implied in the Figure S5b, which is responsible for the enhancement of second emission peaks. Under corresponding optimism excitation wavelength, the PL spectra show the similar profiles with higher intensity of peaks at ~320 nm than that of peaks at ~340 nm (see Figure S5c and d).

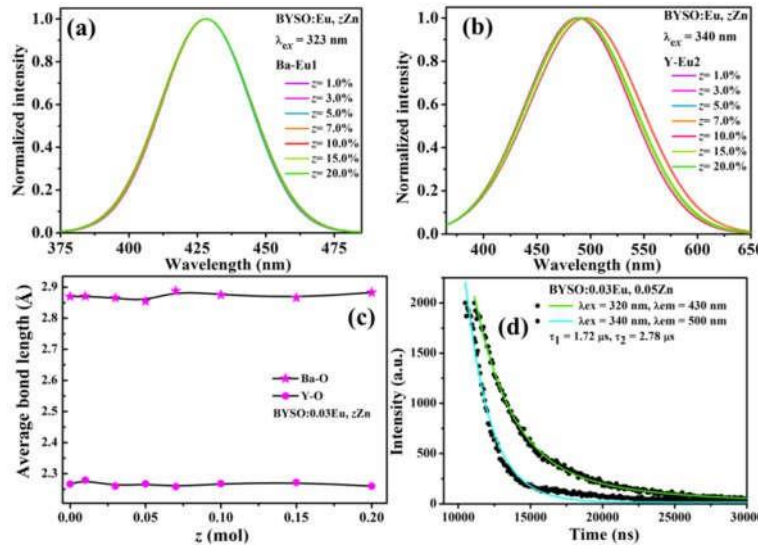


Figure S6. The PL spectra are decomposed into Gaussian contributions from Eu<sup>2+</sup> at the two cation sites in the BYSO:Eu,  $z$ Zn ( $z = 1.0\%-20.0\%$ ), Eu<sup>2+</sup> at the Ba<sup>2+</sup> sites (a), Eu<sup>2+</sup> at the Y<sup>3+</sup> sites (b); the bond length with the various substitution concentrations for Ba-O bond and Y-O bond of BYSO:Eu,  $z$ Zn (c); the corresponding decay curves of the BYSO:0.03Eu<sup>2+</sup>, 0.05Zn<sup>2+</sup> (d).

The Gaussian decomposition results in Figure S6 a and b indicate that there is no peak shifts for Eu(1)<sup>2+</sup> and Eu(2)<sup>2+</sup>, in line with the variation of bond length for Ba-O and Y-O as shown in Figure S6 c. The decay curves of BYSO:0.03Eu<sup>2+</sup>, 0.05Zn<sup>2+</sup> display the characteristic of coexistence of two different kind of Eu<sup>2+</sup> ions with mean decay times of 1.72  $\mu\text{s}$  and 2.78  $\mu\text{s}$  (see Figure S6 d).

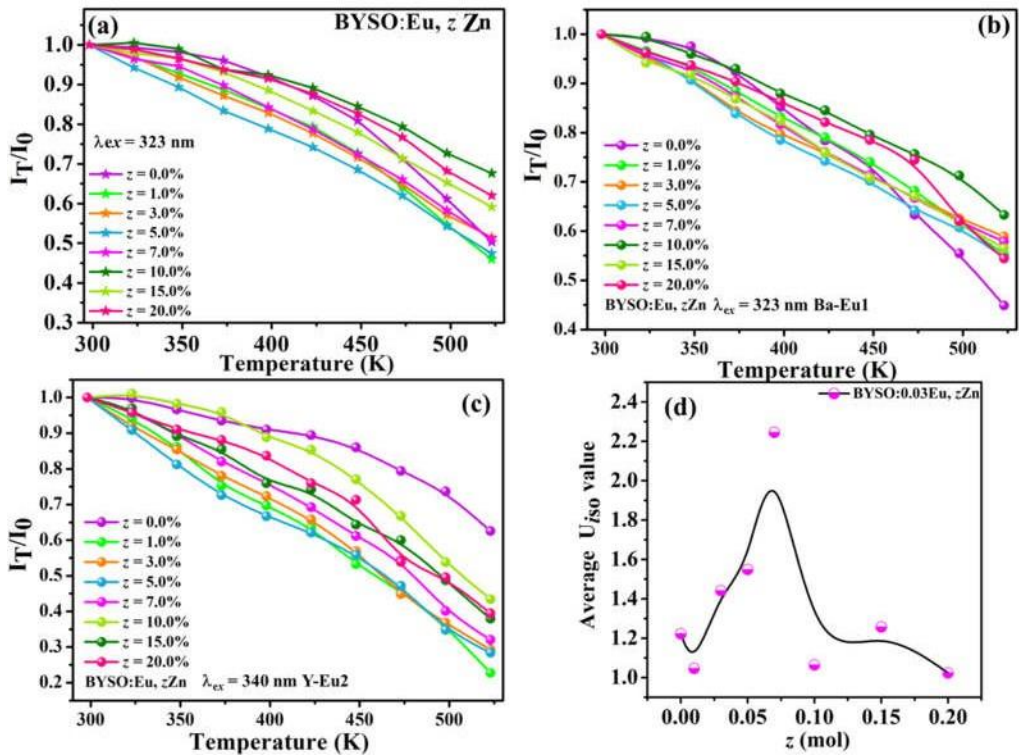


Figure S7. Thermal stability of BYSO:Eu,  $z$ Zn ( $z = 1.0\%-20.0\%$ ) (a); temperature-dependent PL intensity of Eu(1) in  $[\text{BaO}_8]$  polyhedra (under 323 nm) (b) and Eu(2) in  $[\text{YO}_6]$  octahedra (under 340 nm) (c) of BYSO:Eu,  $z$ Zn; concentration-dependence of average  $U_{iso,i}$ values (d).

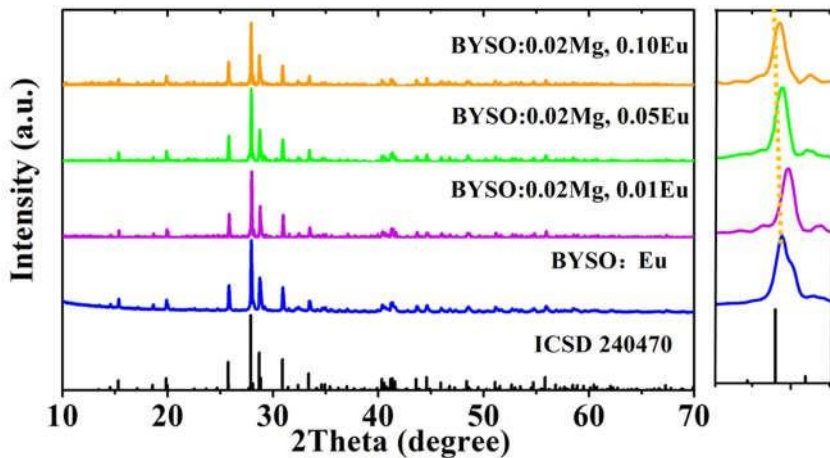


Figure S8. XRD patterns of BMSO:  $n$ Eu,  $n = 0.00-0.10$  and the standard reference

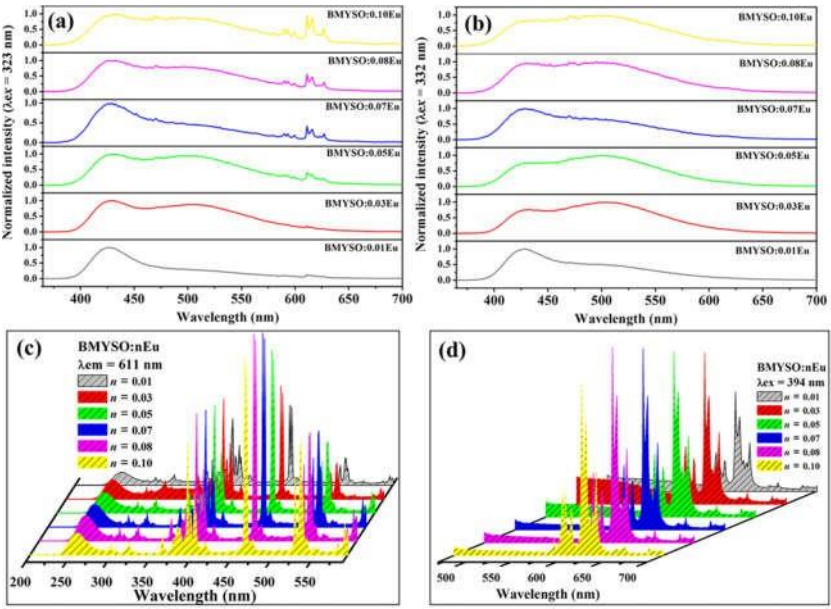


Figure S9. PL spectra of BMYSO:  $n$ Eu ( $n = 0.01\text{--}0.10$ ) excited by  $\sim 320$  nm (a),  $\sim 340$  nm (b),  $394$  nm (d) and PLE spectra monitored at  $611$  nm (c).

When excited by  $320$  nm (Figure S9a), the samples exert growing sharp emission in the range from  $575$  to  $625$  nm with increased Eu contents. We could also find that the characteristic emission of  $\text{Eu}^{2+}$  maintains the efficient broad bands with variation of  $n$ , similar with the samples doped by  $0.03$  mol Eu. The PLE (monitored at  $611$  nm) and PL (excited by  $394$  nm) spectra of BMYSO:  $n$ Eu samples are shown in Figure S9c and d. It is obvious that both of the PLE and PL intensities reach the maximum values at  $n = 0.08$ .

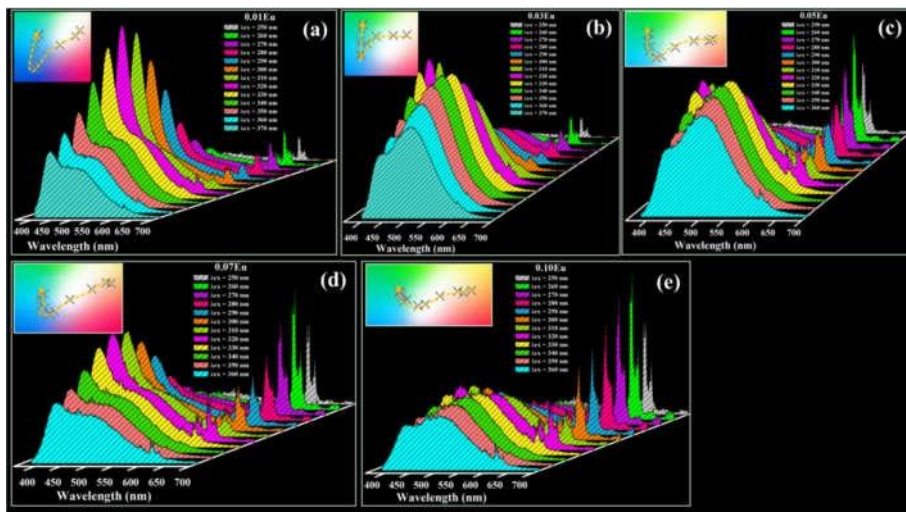


Figure S10. The emission spectra excited by  $250\text{--}360$  nm and the corresponding color coordinates for BMYSO:  $0.01$ Eu (a), BMYSO:  $0.03$ Eu (b), BMYSO:  $0.05$ Eu (c), BMYSO:  $0.07$ Eu (d) and BMYSO:  $0.10$ Eu (e), respectively.